https://dx.doi.org/10.1016/j.proci.2022.07.212

Chemical kinetic interactions of NO with a multi-component gasoline surrogate: experiments and modeling

Song Cheng[a,b,*], Chiara Saggese[c,*], S. Scott Goldsborough[a,*], Scott W. Wagnon [c], William J. Pitz[c]

[a]*Energy Systems Division, Argonne National Laboratory, Lemont, IL 60439, USA*
[b]*Department of Mechanical Engineering, The Hong Kong Polytechnic University, Kowloon, Hong Kong*
[c]*Materials Science Division, Lawrence Livermore National Laboratory, Livermore, CA 94551, USA*

Abstract

This work reports an experimental and modeling study on the chemical kinetic interactions of NO with a multi-component gasoline surrogate, namely PACE-20, using a twin-piston rapid compression machine at a stochiometric fuel loading with 20% EGR (exhaust gas recirculation) by mass, pressures of 20 and 40 bar, and temperatures from 700 to 930 K. Five NO concentrations are investigated, namely 0, 20, 50, 70 and 150 ppm, where NO addition effects are characterized through changes in PACE-20 ignition reactivity and heat release characteristics. Experiments indicate that within the low-temperature regime, NO promotes low-temperature heat release rate and main ignition reactivity at low addition levels, with saturation or even inhibiting effects observed at >50 ppm NO addition, while within the NTC/intermediate-temperature regime, adding NO only promotes reactivity. A recently updated, detailed chemical kinetic model with chemistry specific to NOx/hydrocarbons interaction incorporated is used to simulate the experiments, and reasonable agreement is obtained. In-depth sensitivity and rate of production analyses are further performed. The results indicate that NO interacts with PACE-20 via two types of interaction: (a) direct interactions between NO and PACE-20 derivatives, primarily through $NO+HO_2 \leftrightarrow NO_2+OH$ and $RO_2+NO \leftrightarrow RO+NO_2$, and (b) indirect interactions between PACE-20 derivatives and NO_2 produced from the direct interactions, primarily through $R+NO_2 \leftrightarrow RO+NO$. The observed NO inhibiting effect at low temperatures and 150 ppm NO addition is attributed to the lack of HO_2 radicals to sustain NO consumption via $NO+HO_2 \leftrightarrow NO_2+OH$, and the take-up of inhibiting pathways via $RO_2+NO \leftrightarrow RO+NO_2$. The results also indicate that even with the presence of multiple fuel components, NOx/hydrocarbons interactions are highly selective, and are mainly initiated by the interactions between NO and RO_2 radicals from cyclopentane and ethanol, as well as between NO_2 and R radicals from toluene, 1,2,4-trimethylbenzene and 1-hexene. Further studies on these interactive reactions are therefore highly recommended.

Keywords: chemical kinetic interaction; NOx; multi-component gasoline surrogate; autoignition

*Corresponding authors:

Song Cheng
Email: songcheng@polyu.edu.hk

Chiara Saggese
Email: saggese1@llnl.gov

S Scott Goldsborough
Email: sgoldsborough@anl.gov

1. Introduction

NOx species, including NO, NO_2, N_2O, etc., are minor species that are typically seen in residual and exhaust gases of gasoline-fueled engines. Despite their small in-cylinder concentrations (typically on the order of 10–100 ppm after mixing with fresh charge, or up to 250 ppm with external exhaust gas recirculation (EGR)), they can influence combustion characteristics greatly.

Among these species, NO has attracted the most attention in recent years, and has been reported to have a significant impact on autoignition in both spark-ignition [1-4] and HCCI engines [5-7]. Previous engine studies have reported that NO exhibits promoting effects on gasoline autoignition reactivity at low addition levels (e.g., <500 ppm) [3, 5-7], whereas at higher NO concentrations (e.g., >500 ppm) and low intake temperatures, NO promoting effect starts to saturate and can be even reversed [3, 5]. Understanding the governing chemical kinetics behind these unique behaviors is necessary to the advancement of novel engine technologies. Fundamental reactors, such as rapid compression machines (RCM), shock tubes, flow reactors, etc., are beneficial in this regard.

To date, fundamental studies investigating interactions between NO and typical components of gasoline fuels have already been reported in a flow reactor (for n-pentane [8]), several jet-stirred reactors (for ethanol [9, 10], n-pentane[11-14], n-heptane [15], iso-octane [15], toluene [15], a PRF [5] and a TRF [5]) and several RCMs (for n-heptane [16] and iso-octane [17, 18]), where both inhibiting and promoting effects have been reported, consistent with the aforementioned engine studies. Detailed analyses such as sensitivity and flux analysis have provided further insight into NO interacting chemistry, where it was found that NO promotes and inhibits autoignition reactivity mainly via $NO+HO_2 \leftrightarrow NO_2+OH$ and $RO_2+NO \leftrightarrow RO+NO_2$, respectively.

Though some understandings have been established, gasoline/NO interacting chemistry at engine relevant conditions is still not fully understood. This is mainly due to: (a) the conditions studied so far in fundamental reactors are less representative of advanced combustion engines (e.g., the pressure conditions in the aforementioned fundamental studies are below 20 bar (with the majority below 10 bar), which are lower than pressures experiences in engine cylinder); (b) fundamental studies using representative components of gasoline fuels are scarce, particularly for oxygenates such as ethanol, naphthenes such as cyclopentane, olefins such as hexene and heptene, and aromatics such as toluene and 1,2,4-trimethylbenzene; and (c) to the best of the authors' knowledge, there is no fundamental study on NO interactions with multi-component fuels. Existing fundamental studies are either for single-component or binary fuels, which are less representative of practical gasoline fuels.

Therefore, this study aims to reveal the impacts of NO on the autoignition and preliminary heat release of a multi-component gasoline surrogate fuel at conditions that are more representative of advanced engine operation, and to further the understanding of the underlying chemistry responsible for the observed NO addition effects. Toward this, new measurements are conducted for a complex gasoline surrogate, namely PACE-20, in an RCM with 20% EGR by mass and 0–150 ppm NO at a stochiometric fuel loading, compressed pressure of 20 and 40 bar, and compressed temperature from 700 to 930 K. These conditions are selected to represent conditions in boosted spark-ignition (SI) engines with EGR, which generate NO from high-T flame propagation but have low-T/high-P in the end-gas. Changes in overall ignition reactivity and heat release behavior are both quantified and compared across different NO addition levels. A recently-updated, detailed gasoline surrogate model with specific NO interacting chemistry incorporated is used to model the experiments. In-depth sensitivity and rate of production (ROP) analyses are also performed to provide further insight into the gasoline/NO interacting chemistry.

2. Experimental and computational methods

2.1 Gasoline surrogate

PACE-20 is a high-fidelity, multi-component gasoline surrogate developed for a research-grade, US E10 (10% liquid volume ethanol) gasoline, termed RD5-87. It is formulated targeting a comprehensive set of physical and chemical properties of RD5-87 by a working group of the PACE consortium. Details of the surrogate formulation have been well documented in [19], hence will not be discussed here. The composition and selected properties of PACE-20 and RD5-87 are summarized in Table 1.

Table 1
Percent composition (liquid volume basis) and selected properties of RD5-87 and PACE-20.

	RD5-87	**PACE-20**	
***n*-P**araffins	16.8	*n*-Pentane	14.0
		n-Heptane	11.5
***I**so*-paraffins	32.8	*iso*-Octane	25.0
Olefins	6.7	1-Hexene	5.4
Naphthenes	11.5	Cyclopentane	10.5
Aromatics	22.1	Toluene	9.2
		1,2,4-Trimethylbenzene	11.9
		Tetralin	3.0
o**X**ygenates	10.1	Ethanol	9.6
RON	92.3	92.1	
MON	84.6	84.5	
AKI	88.4	88.3	

* PACE-20 composition in mole fractions is included in Table S1 in the Supplementary Material

2.2 Experimental

2.2.1 RCM description

A heated twin-piston RCM (tpRCM) at Argonne National Laboratory (ANL) is utilized for this study. A detailed description of its configuration and recent modifications, as well as uncertainties associated with measurements can be found in [20, 21], and are briefly described here. A single compression event is driven by a pneumatic system, with a hydraulic ring-groove system used at the end of the stroke to arrest the fast-moving pistons and lock them in place. The reaction chamber pistons utilize crevices machined around their circumference [20] to suppress possible roll-up vortices during the compression, thus improving post-compression charge homogeneity. Electrical-heating tapes are used to heat the reaction chamber to desired temperature, with high-density insulation used to isolate it from the hydraulic chamber. Dynamic pressure is measured using an uncoated, diaphragm-reinforced, thermal-shock resistant Kistler 6045A-U20 pressure transducer calibrated to 250 bar and coupled to a Kistler 5064 charge amplifier.

2.2.2 EGR mixing (excluding NO)

The EGR used in this study is assumed to consist of complete combustion products (N_2, CO_2 and H_2O) at the stoichiometry of one for PACE-20, which is prepared and premixed with the PACE-20/oxidizer mixture in a 5.6 L, stainless steel tank, heated to 70 °C, prior to the experiments. PACE-20 is first introduced into the purged and evacuated tank using a weighed syringe, and the high purity gases are then supplied to the tank in the sequence of Ar (99.9997%, Airgas), N_2 (99.9998%, Airgas) and O_2 (99.9997%, Airgas). Thereafter, liquid H_2O (99.99%) is injected into the mixing tank using another weighed syringe. Then the PACE-20/oxidizer/EGR mixture is isolated for at least 4 hours to diffusively homogenize. The partial pressure of H_2O in the mixture is maintained at <50% of its saturated vapor pressure to ensure no condensation of water during the experiments. Total water evaporation, determined based on the measured water partial pressure and injected water mass, is above 90% for all the experiments.

2.2.3 NO mixing

The test mixture containing NO is prepared in the heated reaction chamber (303–358 K) by feeding the desired amount of NO (supplied with a custom-made N_2 balanced NO cylinder from Airgas with a NO concentration of 2007±2 ppm) and PACE-20/oxidizer/EGR mixture (supplied from the mixing tank) into the reaction chamber. Prior to each NO addition experiment, the NO/N_2 mixture is first filled into the reaction chamber and isolated for 4 minutes. Thereafter, the PACE-20/oxidizer/EGR mixture is filled into the reaction chamber and isolated for 1 minute. Waiting times from 1–4 minutes for both the NO/N_2 mixture and PACE-20/oxidizer/EGR mixture have been evaluated, with no noticeable variation in ignition delay time observed. The uncertainty of NO mole fraction in the test mixture is estimated to be under ±5%, which is calculated using linear uncertainty propagation, following [18], considering the uncertainty in initial filling pressure (±0.25% of 400–1110 Torr), filling pressure of the NO/N_2 mixture (±0.25%), NO mole fraction in N_2 (±2 ppm), and initial temperature (±2.2 K).

2.2.4 Data analysis

Details of data analysis have already been reported in [22], and are briefly described here. The compressed temperature (Tc), main ignition delay time (τ) and heat release rates (HRR) are determined by post-processing recorded reactive and non-reactive pressure traces. To ascertain the end of compression (t_0) and the extent of the heat loss during ignition delay period, a non-reactive test, wherein O_2 in the test mixture is replaced with N_2, is conducted for each reactive condition. Tc is calculated using adiabatic core hypothesis: $\int_{T_i}^{T_c} \frac{\gamma}{\gamma-1}\frac{dT}{T} = \frac{\ln P_c}{P_i}$, where subscripts '$i$' and '$c$' indicate the initial and compressed conditions, and γ is the ratio of specific heats of the mixture, which is estimated as functions of mixture composition (determined based on equilibrium calculation) and temperature using NASA polynomial fits.

An energy balance approach [23] is used to calculate the HRR, and accumulated, or integrated heat release, with assuming ideal gas behavior and uniform pressure across the reaction chamber. Details of the HRR derivation can be found in [24], which can be expressed as,

$$HRR = \frac{\gamma}{\gamma-1}\frac{dV}{dt}[P - P_{nr}] + \frac{1}{\gamma-1}V\left[\frac{dP}{dt} - \left.\frac{dP}{dt}\right|_{nr}\right] - \frac{PV}{(\gamma-1)^2}\left[\frac{d\gamma}{dt} - \left.\frac{d\gamma}{dt}\right|_{nr}\right] \quad (1)$$

where V is the reaction chamber volume, P is the pressure, t denotes time, and the subscript 'nr' indicates non-reacting condition. dV/dt is calculated from non-reactive pressure-time histories using the isentropic relations. The gas temperature during the reactive tests is calculated as, $T \approx T_{nr} + x_b(LHV_{mix}/c_v)$, where LHV_{mix} is the lower heating value of the mixture (calculated based on the initial mixture composition and mass), c_v is the constant-volume specific heat of the mixture, and x_b is the fraction of fuel energy released, which is deduced from $\int(HRR)dt/LHV_{mix}$.

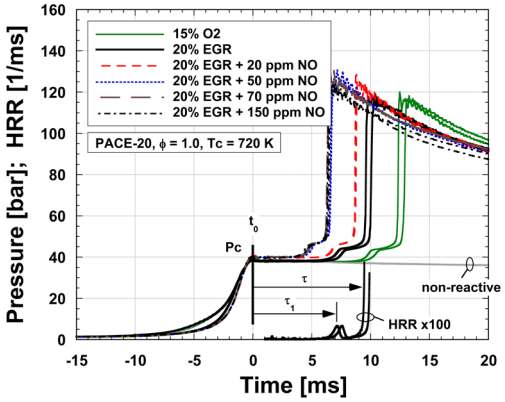

Fig. 1. Representative reactive and non-reactive pressure-time histories of different PACE-20 mixtures at ϕ = 1.0, Pc = 40 bar and Tc = 720 K. The normalized HRR trajectory for the case of 20% EGR and 0 ppm NO is also presented.

Representative reactive and non-reactive pressure-time histories for different PACE-20 mixtures (with and without NO and EGR) at Tc = 720 K and Pc = 40 bar are presented in Fig. 1, where first-stage and main ignition delay times are defined for the case with 20% EGR and 0 ppm NO addition. As can be seen in Fig. 1, at least two tests are conducted at each condition to ensure good repeatability. The corresponding HRR trajectory for the case with 20% EGR and 0 ppm NO addition is also included in Fig. 1, where low-temperature heat release (LTHR) and intermediate-temperature heat release (ITHR), can be determined [25].

An uncertainty analysis associated with ANL's tpRCM is documented in [20], as in [21, 22, 24], leading to ±1.5%, ±10% and ±10% in conservative estimates to Tc, τ and HRR, respectively. Specifically, uncertainty of Tc is estimated also using linear propagation considering the uncertainties in Ti, Pi, Pc and γ, following [26]; that of τ is estimated from data scatter over months, i.e., standard deviation (SD) of repeated measurements. It should be noted that determining the full uncertainty in τ requires utilizing comprehensive uncertainty analysis frameworks, such as [27, 28], which is beyond the scope of this work.

2.2.5 *Test mixtures*

A diluted/stoichiometric operating condition (15.7% O_2, ϕ = 1.0) is considered in this work, with 20% EGR (mass basis) employed, and two different diluents, Ar and N_2, utilized to cover desired Tc ranges (700–930 K). Five different NO concentrations are studied, including 0, 20, 50, 70 and 150 ppm. The test conditions are summarized in Table 2.

Table 2
Summary of test conditions used in this study (gases are presented in mole fraction; NO presented in ppm).

Tc/K	ϕ	PACE-20	O_2	N_2	Ar	CO_2	H_2O	NO/ppm	Pc/bar
< 810	1.0	0.0187	0.1573	0.7726	0	0.0272	0.0247	0–150	20, 40
>810	1.0	0.0187	0.1573	0.2758	0.4966	0.0272	0.0247	0–150	20, 40

2.3 *Modeling*

The kinetic model developed in the work of Cheng et al. [29] combined with the NOx chemistry developed in Fang et al. [18] is adopted for this work. Regarding NOx/hydrocarbons interacting chemistry, new reactions are added for several PACE-20 components, namely ethanol, 1-hexene, 1,2,4-trimethylbenzene and cyclopentane, and for other aromatics, such as benzene, o-xylene and p-xylene, following the reaction classes and related kinetic parameters presented in Fang et al. [18]. It is worth mentioning that the kinetics used for toluene/NOx interactions published in Fang et al. [18] are further validated against ignition delay time experiments of toluene at 12% O_2 and stoichiometry with addition of 0-200 ppm of NO (results are included in a forthcoming paper that's currently under preparation). The measurements were carried out at 25 and 45 bar in the tpRCM at ANL and the agreement between model and experiments is satisfactory across the range of temperature and NO addition studied. The list of NOx interacting reactions added to the chemistry model can be found in Table S2 in the Supplementary Material, as well as in [30], and the kinetic model is attached as Supplementary Material.

Simulations of the RCM experiments are conducted using the LLNL-developed fast-solver Zero-RK [31], using volume-time histories derived from non-reactive tests in order to account for compression and heat loss effects. The non-reactive volume profiles can be found in the Supplementary Materials.

3. Results and discussion

3.1 *Ignition and HRR results*

Figure 2 presents the measured and simulated relative main ignition delay times for the diluted/stochiometric PACE-20/EGR/NO mixtures at five different NO concentrations (0, 20, 50, 70 and 150 ppm) and compressed pressures of 20 and 40 bar. The relative ignition delay time is used to better elucidate the perturbative effects of NO on autoignition reactivity, which is defined as τ/τ_{0ppmNO}, where τ and τ_{0ppmNO} are the ignition delay times for the NO-containing mixtures and the corresponding 0 ppm NO case, respectively. Relative

ignition delay time above 1.0 indicates an inhibiting effect, while values below 1.0 indicate a promoting effect on fuel reactivity. Absolute ignition delay times (both first stage and main, for experimental and model) are presented in Fig. S1 as functions of inverse compressed temperature, and summarized in the Supplementary Materials.

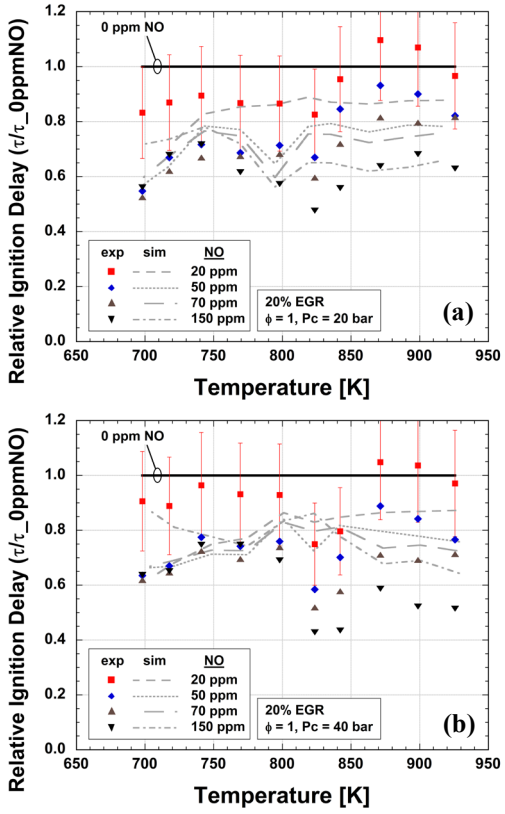

Fig. 2. Measured (color) and simulated (gray) relative main ignition delay times for PACE-20 at $\phi = 1.0$ with 20% EGR by mass and different NO concentrations: (a) Pc = 20 bar; (b) Pc = 40 bar. Argon is used for mixtures with Tc > 810 K.

Similar trends are observed at both 20 and 40 bar in Fig. 2, where NO displays an overall promoting effect on main autoignition reactivity. Additionally, NO also promotes first-stage ignition reactivity, as can be seen in Fig. S1. Though qualitatively consistent, the quantitative effects of NO are somewhat different across different temperature regimes. Specifically, at low temperatures (e.g., Tc < 800 K), the NO promoting effect seems to saturate at 50 ppm, whereas at higher temperatures (e.g., Tc > 825 K), NO keeps promoting fuel reactivity. The change in NO effects across different temperature regimes observed herein for PACE-20 is consistent with previously reported experiments for single-component fuels (e.g., n-heptane [16] and iso-octane [18]). It is also interesting to see that at the lowest temperatures studied (i.e., Tc = 700 K), the charge became less reactive when NO concentration is increased from 70 ppm to 150 ppm, indicating an inhibiting effect of NO at higher concentrations and low temperatures. The same trend has also been observed previously for iso-octane in two RCMs at similar conditions, both with [17] and without EGR [18]. Also worth noting in Fig. 2 is the inhibiting effect of 20 ppm NO at the highest temperature studied, which is observed at both 20 and 40 bar, with slightly greater inhibiting effects exhibited at 20 bar.

To identify NO addition effects on preliminary heat release behavior of PACE-20, the LHV-normalized experimental HRR for PACE-20 with 20% EGR and 0, 70 and 150 ppm NO addition at Pc = 40 bar, Tc = 740 and 900 K are illustrated in Fig. 3. At Tc = 740 K, NO impact on LTHR and ITHR is significant. Compared to the 0 ppm NO case, adding 70 ppm NO promotes the HRR during LTHR (peak value increases from 0.05 to ~0.09 ms^{-1}), leading to faster evolution of ITHR and higher magnitude of peak HTHR (high-temperature heat release). However, when NO concentration is increased to 150 ppm, both the peak HRR and the extent of LTHR are suppressed and become lower than those of the 70 ppm NO case. At Tc = 900 K, NO impact on HRR characteristics is minor.

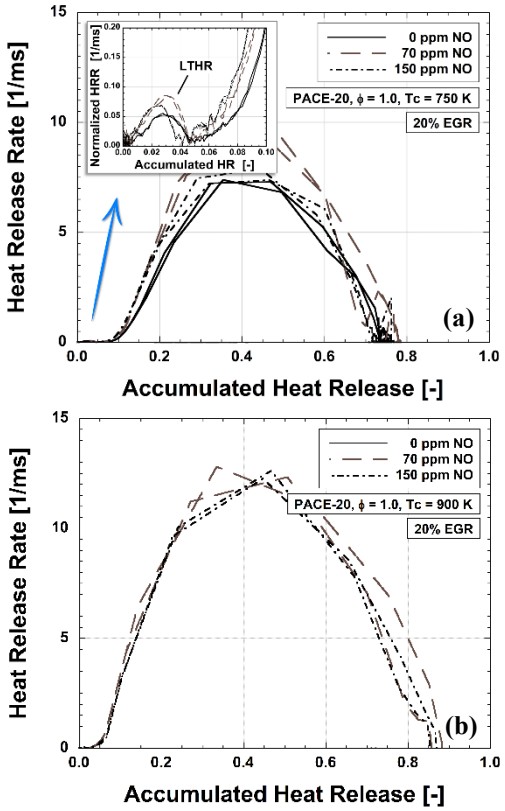

Fig. 3. Normalized experimental heat release rates presented as functions of accumulated heat release for PACE-20 at $\phi = 1.0$, Pc = 40 bar with 20% EGR by mass and different NO concentrations: (a) Tc = 740 K; (b) Tc = 900 K.

Performance of the chemistry model in replicating the experiments is better seen in Fig. S1, where the model captures the global trends of the experiments, including the overall promoting effect of NO on both first-stage and main ignition reactivity at all temperatures, and the inhibiting effect of NO on main ignition reactivity at 150 ppm NO concentration and the lowest temperatures studied. Quantitatively, the model tends to overpredict reactivity at higher temperatures, while underpredicts reactivity at lower temperatures. The largest discrepancies are observed for the 20 ppm NO case. It is important to recognize that the data at 20 ppm were both repeated and reproduced for several times to confirm their fidelity. These discrepancies are mostly due to the insufficiency in NO/PACE-20 interacting chemistry, or PACE-20 chemistry (since similar levels of discrepancies are observed for the 0 ppm NO case), or both. Fundamental experiments representing both EGR presence and small amount of NO additions are needed to validate the kinetic model at these conditions, which are however not available at the moment.

3.2 Sensitivity analysis

Brute force sensitivity analysis on main ignition delay time is conducted for 0, 70 and 150 ppm NO mixtures at Pc = 40 bar and Tc = 740 and 900 K. The sensitivity coefficients are defined as $S_{rel} = \ln\left(\frac{\tau^{\Delta}}{\tau}\right) / \ln\left(\frac{k^{\Delta}}{k}\right)$, where τ^{Δ} and τ are the ignition delay times after multiplying and dividing, respectively, the original rate constant by 2. Figure 4 presents the computed sensitivity coefficients for the top sensitive reactions, where the participating species can be identified in the species dictionary in the Supplementary Materials.

At Tc = 740 K (Fig. 4a), the most sensitive reactions are typical reaction classes within the low-temperature regime, including H-atom abstraction by OH, second O_2 addition to QOOH (hydroperoxyalkyl radical), H_2O_2 decomposition and HO_2 recombination. The influence of NO is also clearly seen in Fig. 4a, where NO promotes reactivity mainly via NO+HO_2↔NO_2+OH, and less significantly via R+NO_2↔RO+NO. The promoting effect somewhat saturates at 70 ppm NO addition, as can be inferred from the similar magnitude of sensitivity coefficients for these promoting reactions between 70 and 150 ppm NO additions, which is consistent with the results observed in Fig. 2. On the other hand, NO also inhibits reactivity via RO_2+NO↔RO+NO_2 pathways, where NO consumes RO_2 radicals that could otherwise lead to low temperature OH branching. These pathways become more influential at higher NO concentrations, as indicated by the increased sensitivity at 150 ppm NO addition compared to 70 ppm NO addition. This explains the trends observed in Figs. 2 and 3a, where 150 ppm NO addition exhibits decreased low-temperature reactivity and LTHR extent than 70 ppm NO addition. It is also interesting to see in Fig. 4a that with NO addition, the sensitivity for two inhibiting reactions, namely CPT+OH↔CYC_5H_9+H_2O and C_2H_5OH+OH↔SC_2H_4OH+H_2O, decrease greatly. These reactions reduce reactivity as their ensuing pathways lead to HO_2 formation rather than OH branching [26], resulting in reduced reactivity at low temperatures. However, with NO presence, the produced HO_2 can be converted to OH via NO+HO_2↔NO_2+OH, making these reactions less inhibiting.

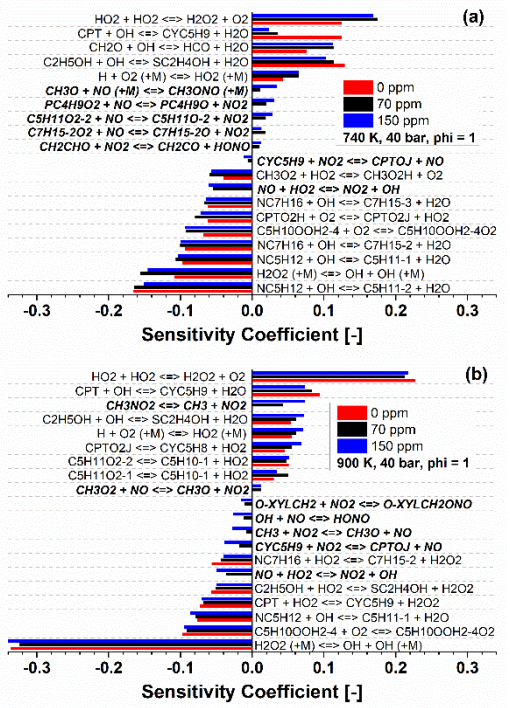

Fig. 4. Sensitivity analysis on main ignition delay times for PACE-20 at ϕ = 1.0 and Pc = 40 bar with 20% EGR by mass and different NO concentrations: (a) Tc = 740 K; (b) Tc = 900 K. NO interacting reactions are highlighted in ***italic***.

At Tc = 900 K (Fig. 4b), NO promoting reactions become more expressive than the inhibiting ones, with NO+HO_2↔NO_2+OH still being the top promoting reaction from NO interaction. Compared to Tc = 740 K, NO promoting effect via R+NO_2↔RO+NO pathways become more pronounced at this temperature. Unlike the trends observed at 740 K where the NO promoting reactions demonstrate similar sensitivities at both 70 and 150 ppm NO additions, the NO promoting reactions at 900 K become more influential with further increased NO concentration. This aligns well with the results in Fig. 2, where NO keeps promoting reactivity without showing saturation effect at NTC (negative temperature coefficient) to intermediate temperatures. Additionally, without sufficient RO_2 production at this temperature, NO addition can still contribute to

its inhibiting effect via $CH_3NO_2 \leftrightarrow CH_3+NO_2$. This reaction occurs in the reverse direction and inhibits reactivity as it competes with the promoting reaction $CH_3+NO_2 \leftrightarrow CH_3O+NO$. This could be related to the NO inhibiting effect at 20 ppm and high temperatures observed in Fig. 2. Whether this is the case requires further investigation.

3.3 Rate of production (ROP) analysis

ROP analysis is further carried out for NO and NO_2 at 2% n-heptane consumption for the 70 and 150 ppm NO addition cases at the same conditions as in Fig. 4. 2% n-heptane consumption is selected to track NO interaction pathways at the start of the oxidation process. NO and NO_2 are selected due to their dominant role in contributing to NO addition effects, as seen in Fig. 4. The results covering only the most dominant pathways are presented in Fig. 5.

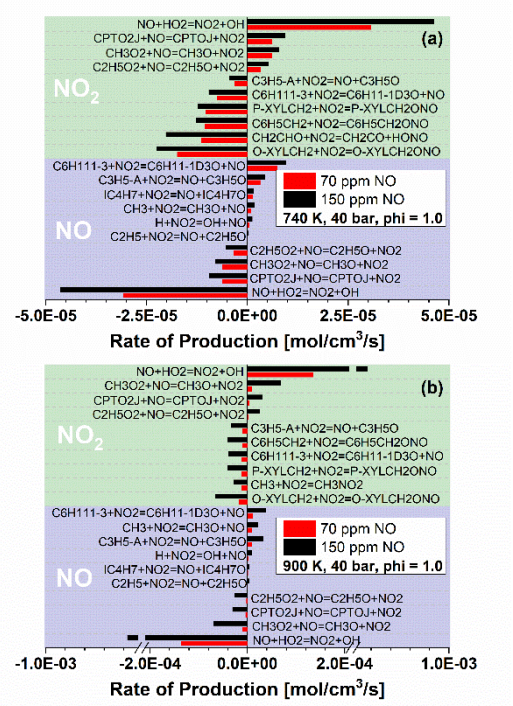

Fig. 5. ROP analysis of NO and NO_2 at 2% n-heptane consumption for PACE-20 at ϕ = 1.0 and Pc = 40 bar with 20% EGR by mass and different NO concentrations: (a) Tc = 740 K; (b) Tc = 900 K.

At Tc = 740 K (Fig. 5a), NO addition effects are initiated by two types of interaction: (a) direct interactions between NO and derivatives from PACE-20, and (b) interactions between PACE-20 derivatives and NO_2 produced from NO consuming pathways. As can been seen in Fig. 5a, NO is consumed via interactive reactions mostly by HO_2 radical and less significantly by RO_2 radicals, with both leading to the formation of NO_2. The interaction between NO and HO_2 greatly promotes reactivity, as seen in Fig. 4, since it converts the less reactive HO_2 radicals to highly reactive OH radicals. Despite the presence of multiple RO_2 radicals from PACE-20 oxidation, NO interactions with RO_2 radicals are highly selective and are not proportional to the concentrations of different PACE-20 components. Specifically, at the initial oxidation stage, NO interacts the most with $CPTO_2J$ and CH_3O_2, which are products from CPT and mostly from ethanol at this stage [32], respectively. On the other hand, the produced NO_2 from direct NO interactions mainly participates in interactive reactions with resonantly-stabilized R radicals mostly from 1,2,4-trimethylbenzene (e.g., $O\text{-}XYLCH_2+NO_2$ and $P\text{-}XYLCH_2+NO_2$), then toluene (e.g., $C_6H_5CH_2+NO_2$) and less significantly 1-hexene ($C_6H_{11}1\text{-}3+NO_2$). These pathways promote reactivity as they consume unreactive resonantly-stabilized radicals and lead to the formation of NO that can further contribute to OH production via $NO+HO_2 \leftrightarrow NO_2+OH$. Comparing 150 ppm NO addition with 70 ppm NO addition, it is seen that increasing NO concentration leads to increase in ROP for all consuming and producing pathways for both NO and NO_2. The increase in the consuming and producing pathways counteract each other, leading to similar net ROP between the 70 and 150 ppm NO addition cases.

At Tc = 900 K (Fig. 5b), the top consuming and producing reactions at the initial stage of the oxidation process are similar to those at Tc = 740 K, where NO interacts mostly with HO_2, then with CH_3O_2 and $CPTO_2J$, and NO_2 interacts primarily with the primary fuel radicals from aromatics and 1-hexene. However, at this temperature, the contribution of $NO+HO_2 \leftrightarrow NO_2+OH$ to NO consumption and NO_2 production is significantly greater than other contributing pathways (i.e., ROP for $NO+HO_2 \leftrightarrow NO_2+OH$ is greater than others by over 10 times, vs. ~4 times at Tc = 740 K). Also different from Tc = 740 K is the considerably increased ROP for all contributing pathways when NO is increased from 70 to 150 ppm, particularly for $NO+HO_2 \leftrightarrow NO_2+OH$, where the ROP is increased by nearly 8 times (vs. only ~1.5 times at Tc = 740 K). These trends are due mostly to the increased production of HO_2 at this temperature compared to Tc = 740 K. The increased ROP via $NO+HO_2 \leftrightarrow NO_2+OH$ at 150 ppm NO addition enhances the ROP for OH and, subsequently, for all $R+NO_2$ pathways that further produce NO, resulting in a further increased fuel reactivity compared to that with 70 ppm NO addition (Fig. 2).

4. Conclusion

NO addition effects on the autoignition and heat release characteristics of a multi-component gasoline surrogate (PACE-20) are investigated in ANL's tpRCM using experimental and numerical frameworks at five NO concentrations (0, 20, 50, 70 and 150 ppm) under a stoichiometric fuel loading with

20% EGR by mass, pressures of 20 and 40 bar, and temperatures from 700 to 930 K.

Experiments indicate that within the low-temperature regime, NO promoting effect on both LTHR and autoignition reactivity of PACE-20 is strong at ≤50 ppm NO addition, starts to saturate at 70 ppm NO addition, and is reversed at 150 ppm NO addition, whereas within the NTC/intermediate-temperature regime, adding NO keeps promoting autoignition reactivity without exhibiting any saturation effect. These trends are reasonably well captured by the chemical kinetic model.

Sensitivity and ROP analysis results clearly highlight the importance of NOx/PACE-20 interacting pathways in contributing to the observed NO addition effects, particularly the direct interactions between NO and PACE-20 derivatives via $NO+HO_2 \leftrightarrow NO_2+OH$ and $RO_2+NO \leftrightarrow RO+NO_2$, and the indirect interactions between PACE-20 derivatives and NO_2 produced from the direct interactions via $R+NO_2 \leftrightarrow RO+NO$. With the multi-component surrogate, there exists a competing mechanism between different fuel components in NO and NO_2 participating pathways, which considerably complicates the underlying interacting chemical kinetics. At high NO addition levels, the global NO addition effects at different temperatures result from competition between the promoting and inhibiting interacting pathways. For instance, with 150 ppm NO addition, the NO inhibiting effect at Tc = 740 K is caused by the lack of HO_2 radicals to sustain NO consumption via the top promoting pathway $NO+HO_2 \leftrightarrow NO_2+OH$, and the take-up of inhibiting pathways via $RO_2+NO \leftrightarrow RO+NO_2$, whereas at Tc = 900 K where HO_2 is sufficiently produced, NO promotes reactivity since NOx/PACE-20 interactions are still dominated by $NO+HO_2 \leftrightarrow NO_2+OH$.

Even with the presence of multiple fuel components, NOx/hydrocarbons interactions are highly selective, and NO addition effects are mainly initiated by the interactions between NO and RO_2 radicals from cyclopentane and ethanol, as well as between NO_2 and R radicals from toluene, 1,2,4-trimethylbenzene and 1-hexene. Further studies on these interactive reactions are highly recommended.

Acknowledgement

The work at ANL and LLNL were supported by the U.S. Department of Energy PACE Initiative with Gurpreet Singh and Michael Weismiller as program managers, under contract No. DE-AC02-06CH11357 and DE-AC52-07NA27344, respectively.

Supplementary material

SMM1 includes the first-stage and main IDT results; SMM2 lists the species identifiers; SMM3 is the mechanism file in CHEMKIN format; SMM4 is the thermochemistry file in CHEMKIN format; SMM5 summarizes all experimental data; and SMM6 contains all non-reactive volume profiles.

References

[1] S. Cheng, Y. Yang, M.J. Brear, D. Kang, S. Bohac, A.L. Boehman, Autoignition of pentane isomers in a spark-ignition engine, Proc. Combust. Inst. 36 (2017) 3499-3506.

[2] P.J. Roberts, C.G.W. Sheppard, The Influence of Residual Gas NO Content on Knock Onset of Iso-Octane, PRF, TRF and ULG Mixtures in SI Engines, Int. J. Engine Res. 6 (2013) 2028-2043.

[3] Z. Chen, H. Yuan, T.M. Foong, Y. Yang, M. Brear, The impact of nitric oxide on knock in the octane rating engine, Fuel 235 (2019) 495-503.

[4] A.A. Burluka, K. Liu, C.G.W. Sheppard, A.J. Smallbone, R. Woolley, The influence of simulated residual and NO concentrations on knock onset for PRFs and gasolines, SAE Transactions 113 (2004) 1873-1889.

[5] A. Dubreuil, F. Foucher, C. Mounaı¨m-Rousselle, G. Dayma, P. Dagaut, HCCI combustion: Effect of NO in EGR, Proc. Combust. Inst. 31 (2007) 2879-2886.

[6] J.-B. Masurier, F. Foucher, G. Dayma, P. Dagaut, Investigation of iso-octane combustion in a homogeneous charge compression ignition engine seeded by ozone, nitric oxide and nitrogen dioxide, Proc. Combust. Inst. 35 (2015) 3125-3132.

[7] F. Contino, F. Foucher, P. Dagaut, T. Lucchini, G. D'Errico, C. Mounaïm-Rousselle, Experimental and numerical analysis of nitric oxide effect on the ignition of iso-octane in a single cylinder HCCI engine, Combust. Flame 160 (2013) 1476-1483.

[8] M. Hori, Y. Koshiishi, N. Matsunaga, P. Glaude, N. Marinov, Temperature dependence of NO to NO2 conversion by n-butane and n-pentane oxidation, Proc. Combust. Inst. 29 (2002) 2219-2226.

[9] M.U. Alzueta, J.M. Hernández, Ethanol Oxidation and Its Interaction with Nitric Oxide, Energy Fuels 16 (2002) 166-171.

[10] M. Abián, C. Esarte, Á. Millera, R. Bilbao, M.U. Alzueta, Oxidation of Acetylene−Ethanol Mixtures and Their Interaction with NO, Energy Fuels 22 (2008) 3814-3823.

[11] H. Zhao, L. Wu, C. Patrick, Z. Zhang, Y. Rezgui, X. Yang, G. Wysocki, Y. Ju, Studies of low temperature oxidation of n-pentane with nitric oxide addition in a jet stirred reactor, Combust. Flame 197 (2018) 78-87.

[12] H. Zhao, A.G. Dana, Z. Zhang, W.H. Green, Y. Ju, Experimental and modeling study of the mutual oxidation of N-pentane and nitrogen dioxide at low and high temperatures in a jet stirred reactor, Energy 165 (2018) 727-738.

[13] L. Marrodán, Y. Song, M. Lubrano Lavadera, O. Herbinet, M. de Joannon, Y. Ju, M.U. Alzueta, F. Battin-Leclerc, Effects of Bath Gas and NOx Addition on n-Pentane Low-Temperature Oxidation in a Jet-Stirred Reactor, Energy Fuels 33 (2019) 5655-5663.

[14] L. Marrodán, Y. Song, O. Herbinet, M.U. Alzueta, C. Fittschen, Y. Ju, F. Battin-Leclerc, First detection of a key intermediate in the oxidation of fuel + NO systems: HONO, Chem. Phys. Lett. 719 (2019) 22-26.

[15] G. Moréac, P. Dagaut, J.F. Roesler, M. Cathonnet, Nitric oxide interactions with hydrocarbon oxidation in a jet-stirred reactor at 10 atm, Combust. Flame 145 (2006) 512-520.

[16] Z. Chen, P. Zhang, Y. Yang, M.J. Brear, X. He, Z. Wang, Impact of nitric oxide (NO) on n-heptane autoignition in a rapid compression machine, Combust. Flame 186 (2017) 94-104.

[17] Y. Song, Y. He, Y. Yu, B. Moreau, F. Foucher, Effect of Exhaust Gas Recirculation and NO on Ignition Delay Times of Iso-octane in a Rapid Compression Machine, Energy Fuels 34 (2020) 8788-8795.

[18] R. Fang, C. Saggese, S.W. Wagnon, A.B. Sahu, H.J. Curran, W.J. Pitz, C.-J. Sung, Effect of nitric oxide and exhaust gases on gasoline surrogate autoignition: iso-octane experiments and modeling, Combust. Flame 236 (2022) 111807.

[19] S. Cheng, S.S. Goldsborough, S.W. Wagnon, R. Whitesides, M. McNenly, W.J. Pitz, D. Lopez-Pintor, J.E. Dec, Replicating HCCI-like autoignition behavior: what gasoline surrogate fidelity is needed?, App. Energy Combust. Sci., under review, (2022).

[20] A. Fridlyand, S.S. Goldsborough, M. Al Rashidi, S.M. Sarathy, M. Mehl, W.J. Pitz, Low temperature autoignition of 5-membered ring naphthenes: Effects of substitution, Combust. Flame 200 (2019) 387-404.

[21] T. Rockstroh, A. Fridlyand, S. Ciatti, W. Cannella, S.S. Goldsborough, Autoignition behavior of a full boiling-range gasoline: Observations in RCM and GCI engine environments, Combust. Flame 209 (2019) 239-255.

[22] S. Cheng, D. Kang, A. Fridlyand, S.S. Goldsborough, C. Saggese, S. Wagnon, M.J. McNenly, M. Mehl, W.J. Pitz, D. Vuilleumier, Autoignition behavior of gasoline/ethanol blends at engine-relevant conditions, Combust. Flame 216 (2020) 369-384.

[23] J.B. Heywood, Internal combustion engine fundamentals, McGraw-Hill, New York, 1988.

[24] S.S. Goldsborough, J. Santner, D. Kang, A. Fridlyand, T. Rockstroh, M.C. Jespersen, Heat release analysis for rapid compression machines: Challenges and opportunities, Proc. Combust. Inst. 37 (2019) 603-611.

[25] S. Cheng, S.S. Goldsborough, S.W. Wagnon, W.J. Pitz, Probing intermediate temperature heat release in autoignition of C3-C4 iso-alcohol/gasoline blends, Combust. Flame 233 (2021) 111602.

[26] S. Cheng, D. Kang, S.S. Goldsborough, C. Saggese, S. Wagnon, W.J. Pitz, Experimental and modeling study of C2-C4 alcohol autoignition at intermediate temperature conditions, Proc. Combust. Inst. 38 (2021) 709-717.

[27] A. Fridlyand, M.S. Johnson, S.S. Goldsborough, R.H. West, M.J. McNenly, M. Mehl, W.J. Pitz, The role of correlations in uncertainty quantification of transportation relevant fuel models, Combust. Flame 180 (2017) 239-249.

[28] S. Cheng, Y. Yang, M.J. Brear, M. Frenklach, Quantifying uncertainty in kinetic simulation of engine autoignition, Combust. Flame 216 (2020) 174-184.

[29] S. Cheng, C. Saggese, D. Kang, S.S. Goldsborough, S.W. Wagnon, G. Kukkadapu, K. Zhang, M. Mehl, W.J. Pitz, Autoignition and preliminary heat release of gasoline surrogates and their blends with ethanol at engine-relevant conditions: Experiments and comprehensive kinetic modeling, Combust. Flame 28 (2021) 57-77.

[30] S. Cheng, C. Saggese, S.S. Goldsborough, S.W. Wagnon, W.J. Pitz, Unraveling the role of EGR olefins at advanced combustion conditions in the presence of nitric oxide: ethylene, propene and iso-butene, Combust. Flame, under review, (2022).

[31] M.J. McNenly, R.A. Whitesides, D.L. Flowers, Faster solvers for large kinetic mechanisms using adaptive preconditioners, Proc. Combust. Inst. 35 (2015) 581-587.

[32] S. Cheng, S.S. Goldsborough, C. Saggese, S.W. Wagnon, W.J. Pitz, New insights into fuel blending effects: intermolecular chemical kinetic interactions affecting autoignition times and intermediate-temperature heat release, Combust. Flame 233 (2021) 111559.